A SEMI-AUTOMATIC METHOD FOR INDIRECT ORIENTATION OF AERIAL IMAGES USING GROUND CONTROL LINES EXTRACTED FROM AIRBORNE LASER SCANNER DATA

Daniel Rodrigues dos Santos[1], Antonio Maria Garcia Tommaselli[2], Quintino Dalmolin[1], Edson Aparecido Mitishita[1]

1 : Universidade Federal do Paraná
Department of Geomatic, Caixa Postal 19001, Centro Politécnico, s/n
CEP 81531-990, Curitiba - Brasil
danielsantos@ufpr.br;dalmolin@ufpr.br;mitishita@ufpr.br

2 : Universidade. Estadual Paulista
Department of Cartography, Caixa Postal 266, Rua Roberto Simonsen, 305
CEP 19060-900, Presidente Prudente - Brasil
tomaseli@fct.unesp.br

Résumé

Cet article présente une méthode d'orientation indirecte d'images aériennes utilisant des lignes d'appui extraites des données d'un système laser aéroporté. Cette stratégie d'intégration de données a démontré son potentiel pour l'automatisation des travaux photogrammétriques, y compris pour l'orientation indirecte des images. La principale caractéristique de l'approche proposée est la possibilité de calculer automatiquement les paramètres d'orientation externe d'une ou plusieurs images au moyen d'une résection spatiale avec des données issues de différents capteurs. La méthode proposée procède comme suit. Les lignes droites sont d'abord extraites automatiquement dans l'image aérienne (s) et dans l'image d'intensités issues des données laser (S). La correspondance entre les lignes de s et S est ensuite établie de manière automatique. Un modèle de coplanarité permet d'estimer les paramètres d'orientation externe de la caméra grâce à un filtre de Kalman étendu itératif IEKF). La méthode a été développée et testée en utilisant des données de différents capteurs. Des expériences ont été réalisées pour évaluer la méthode proposée. Les résultats obtenus montrent que l'estimation des paramètres d'orientation externe est fonction de la précision de localisation du système laser.

Mots clés : laser aéroporté, orientation indirecte, lignes d'appui, IEKF, modèle de coplanarité à partir de lignes.

Abstract

This paper presents a method for indirect orientation of aerial images using ground control lines extracted from airborne Laser system (ALS) data. This data integration strategy has shown good potential in the automation of photogrammetric tasks, including the indirect orientation of images. The most important characteristic of the proposed approach is that the exterior orientation parameters (EOP) of a single or multiple images can be automatically computed with a space resection procedure from data derived from different sensors. The suggested method works as follows. Firstly, the straight lines are automatically extracted in the digital aerial image (s) and in the intensity image derived from an ALS data-set (S). Then, correspondence between s and S is automatically determined. A line-based coplanarity model that establishes the relationship between straight lines in the object and in the image space is used to estimate the EOP with the iterated extended Kalman filtering (IEKF). Implementation and testing of the method have employed data from different sensors. Experiments were conducted to assess the proposed method and the results obtained showed that the estimation of the EOP is function of ALS positional accuracy.

***Keywords** : ALS data-set, indirect orientation, ground control lines, IEKF, line-based coplanarity model.*

Resumo

Este artigo apresenta um método indireto para orientação de imagens digitais usando linhas retas como apoio de campo extraídas do conjunto de dados derivado do sistema de varredura Laser aerotransportado. A estratégia de integração de dados tem mostrado seu potencial na automação de tarefas fotogramétricas, incluindo a orientação de imagens. A característica mais importante da abordagem proposta é que os parâmetros de orientação exterior de uma única ou múltiplas imagens pode ser automaticamente calculada por meio do processo de resseção espacial derivado de dados provenientes de diferentes sensores. Primeiramente, linhas retas são automaticamente extraídas na imagem digital (s) e na imagem de intensidade do pulso Laser (S). Posteriormente, a correspondência entre as feições é automaticamente determinada. O modelo dos planos equivalentes é usado para estimar os parâmetros de orientação exterior da câmera, juntamente com o filtro de Kalman iterativo e extendido (IEKF). Foram implementados algoritmos computacionais e conduzidos testes com dados reais derivados de diferentes sensores. Os resultados obtidos mostraram que a qualidade na estimativa dos parâmetros de orientação exterior é influenciada pela qualidade posicional dos dados do sistema de varredura Laser aerotransportado.

1. Introduction

The indirect orientation of images is still required in different mapping tasks, such as map revision and production, orthophoto and digital terrain model (DTM) generation, 3D extraction and object reconstruction, geographic information system (GIS) updating, change detection, etc.

Nowadays, there are three kinds of orientation methods: direct orientation, indirect and integrated orientation of images. The direct orientation of images is based on the integration of additional orientation sensors, such as global positioning system (GPS) and inertial navigation system (INS), which provides camera position and attitude in each instant of image acquisition. For high accuracy, however, this strategy also requires the use of ground control entities to calculate and correct systematic errors that arise when using GPS and INS (integrated sensor orientation).

The aim of indirect orientation is to establish the relationship between the image and ground reference systems. Various sensor models have been used in indirect methods of image orientation such as the collinearity equations, point-based and line-based coplanarity equations. The idea of using linear features in indirect orientation of images is not new. (Lugnani, 1980) demonstrated the viability of using digital entities as control information. In the last years several researches focusing on the use of linear features in photogrammetric procedures have been presented (Kubik, 1988; Mulawa and Mikhail, 1988; Tommaselli and Lugnani, 1988; Roberts, 1988; Lui et al., 1990; Heikkila, 1991; Heuvel, 1997; Habib, 1999; Schenck, 2004; Zhang, 2004)

According to (Kubik, 1988) and (Tommaselli and Tozzi, 1996), a straight line representation is suitable for the indirect orientation problem due to the following reasons: images of man-made environments contain many straight lines; straight line parameters can be obtained with sub-pixel accuracy; are easier to detect than distinct points; these features can be used in all photogrammetric tasks such as space intersection, resection and triangulation.

Several methods of automatic orientation of images have been proposed: (Sanfeliu and Fu, 1983; Liu et al., 1990; Shapiro and Brady, 1992; Vosselman, 1992; Sclaroff and Pentland, 1993; Tommaselli and Tozzi, 1996; Dal Poz and Tommaselli, 1996; Park et al., 2000; Shan, 2001).

Since the nineties, technologies of light detection and ranging (LiDAR) and airborne laser scanner systems (ALS) have been developed, making feasible the fast generation of digital surface models (DSM) with sparse ground control (Wehr and Lohr, 1999). These technologies can also be used as an alternative for ground control lines (GCL) and ground control points (GCP) data collection. An advantage of these systems is the spectral information acquired by the ALS, which can be employed to produce an intensity image of the reflected pulse.

According to (Habib et al., 2007), the integration of data derived from different acquisition systems has great potential, principally because ALS has the capability to rapidly provide 3D information about points located on a surface with high accuracy and provides rich geometrical surface information, which could complement information from photogrammetric data. Several scientific papers have presented alternative solutions for extracting control points from photogrammetry and ALS data integration, such as: (Habib et al., 2004; Furkuo and King, 2004; Chen et al., 2004; Habib et al., 2007; Mitishita et al., 2008; Santos et al., 2010).

This work presents a semi-automatic method for indirect orientation of aerial images using GCL extracted from the optical images and ALS data-sets. The most important characteristics of the proposed method are related to the following reasons: compared to distinct GCP, GCL have higher semantic content; they are better defined geometrically than individual point occurrences. They are easily detected, recognized and identified from any type of high-resolution imagery and with several different orientations. Considering that accurate GPS/INS systems are expensive and the conventional ground control points survey is time-consuming and also expensive, GCL can be used as rich control information for digital images orientation, mainly because they can be extracted from different ALS dataset, using segmentation algorithms. We can also mention that in the proposed approach pre-signalized ground controls are not needed.

This paper is organised as follows: the method is presented in the next section, followed by the experimental results, discussion, some conclusions and recommendations for future work.

2. Method

2.1. Overview

As described above, the proposed method is based on straight lines derived from different sensors data aiming at the indirect orientation of a digital image. The sequence of processing is:

(1) Automatic extraction of straight lines in both images (optical frame image and ALS intensity image) using an automatic feature extraction algorithm;
(2) Manual correspondence establishment for four straight lines to compute the approximated EOP using the line-based coplanarity model, with conventional least squares adjustment;
(3) Then, each GCL is projected to the image space (reference space for correspondence establishment) using the collinearity equations with the initial EOP computed in the stage 2;
(4) The relational matching (Dal Poz and Tommaselli, 1998), process is used to automatically establish correspondences between the straight lines extracted in the digital image and the GCL projected to reference space;
(5) Then, the straight lines extracted in the digital image and the corresponding GCL are used to compute the orientation of the digital image using the line-based coplanarity model with the IEKF recursive solution. The algorithm repeats stages (4) and (5) continuously until the last available GCL;
(6) Finally, the results obtained are statistically verified.

In the following sections, the methodology and mathematical models used are described in details.

2.2. Feature extraction algorithm

An automatic feature extraction algorithm was used to extract straight lines both on the digital aerial and intensity images. The data flow of this step is composed by smoothing, segmentation, thinning, edge linking, and least square adjustment to fit a straight line to the segmented edges (Sonka et al., 1998; Sahoo et al., 1993; Venkateswar and Chellappa, 1992).

For each straight line extracted in the image space a set of parameters is determined, such as: a and p or b and q (depending on the straight line orientation); their standard deviations (σ_a and σ_p or σ_b and σ_q); and the endpoints coordinates of straight lines extracted in the image space (x_1, y_1, x_2, y_2) and defined in the image space (see section 2.3). For each GCL extracted in the laser intensity image their endpoints coordinates in *C* (Colum) and *L* (Row) are recorded into the digital file coordinates. Then, the corresponding *XYZ* coordinates in the raw data file (non-interpolated scanned points) derived directly from ALS. In order to assign the three-dimensional coordinates to the endpoints of each GCL, two steps are required: first, the extracted coordinates *C* and *L* in the intensity image are transformed to approximated coordinates X^a and Y^a using Equations 1:

$$X^a = X_{or} + (C-1).GSD \qquad (1)$$
$$Y^a = Y_{or} - (L-1).GSD$$

where X_{or} and Y_{or} are the ground coordinates corresponding to the origin of the intensity image and GSD is the ground sample distance (pixel size on the ground).

After this linear transformation for each GCL endpoint (with calculated X^a and Y^a given by Equation 1) the algorithm defines a search circle with a radius of 80 cm to look for corresponding *XYZ* coordinates in the raw data file. The Euclidian distance between all *XY* coordinates within this region and X^aY^a are computed. The smallest distance value is selected and, the *XYZ* coordinates are assigned to the one of the endpoints of a GCL. The process is repeated for the second endpoint and for all the extracted GCL. Finally, the direction vector $\vec{d}$ (see Figure 2) for each GCL with *XYZ* coordinates is computed.

2.3. Initial estimate of EOP

After all the GCL had been automatically extracted in the intensity and digital image, and their three-dimensional coordinates assigned, the correspondence of four straight lines are manually established to compute the approximated EOP using the line-based coplanarity model, proposed by (Tommaselli and Tozzi, 1996) with the conventional least squares adjustment.

The line-based coplanarity model is based on the equivalence between the vector normal to the interpretation plane in the image space and the vector normal to the rotated interpretation plane in the object space. The geometry of the line-based coplanarity model is depicted in Figure 1.

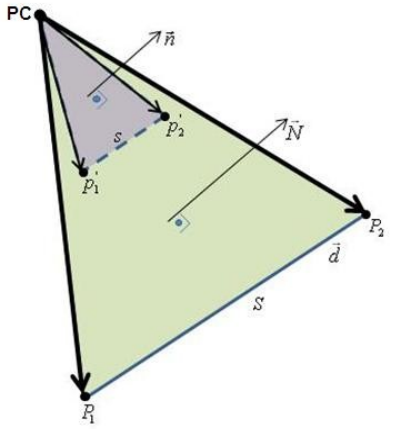

Figure 1: Geometry of the line-based coplanarity model.

P_1P_2 are the endpoints of straight lines extracted in the laser intensity image (with XYZ coordinates assigned from points in the original cloud in object space), p_1p_2 are the endpoints of straight lines extracted in the digital frame image (image space). In Figure 1, the interpretation plane contains the straight line in the object space (*S*), the projected straight line in the image space (s), PC is the perspective center (with coordinates X_o, Y_o, Z_o) and $\vec{d}$ the direction vector of a straight line.

The vector $\vec{n}$ defines the normal vector to the interpretation plane in the image space and the vector $\vec{N}$ the normal vector to the interpretation plane in the object space. Multiplying the vector $\vec{N}$ by the Rotation Matrix (*R)*, defined by the sequence $R = R_\kappa R_\varphi R_\omega$, and by scale factor ($\lambda$) can be written the model in its basic form, as follows:

$$\vec{n} = \lambda \vec{N} R \qquad (2)$$

In Equation (2) carrying out some mathematical manipulations we have the line-based coplanarity model as follows:

$$a = -\frac{r_{11}.nx + r_{12}.ny + r_{13}.nz}{r_{21}.nx + r_{22}.ny + r_{23}.nz}$$
$$p = -c\frac{r_{31}.nx + r_{32}.ny + r_{33}.nz}{r_{21}.nx + r_{22}.ny + r_{23}.nz} \qquad (3)$$

a and *p* are the straight line parameters for intervals 45°<θ<135° or 225°<θ<335°, *c* is the calibrated focal length, n_x, n_y, and n_z are the elements defined by the cross product between $\vec{d}$ and the vector difference $\overrightarrow{PCP_1}$; $r_{11}...r_{33}$ are the elements of the Rotation Matrix *R*.

In order to avoid divisions by zero, another equation can be written as follows:

$$b = -\frac{r_{21}.nx + r_{22}.ny + r_{23}.nz}{r_{11}.nx + r_{12}.ny + r_{13}.nz}$$
$$q = -c\frac{r_{31}.nx + r_{32}.ny + r_{33}.nz}{r_{11}.nx + r_{12}.ny + r_{13}.nz} \qquad (4)$$

b and *p* are the straight line parameters for intervals 45°<θ<135° or 135°<θ<225° or 315°<θ<360°. The

variances of the straight line parameters can be obtained as follows:

$$\sigma_a^2 = \frac{2(a^2+1)}{(x_2-x_1)^2}\sigma_{xy}^2 \qquad (5)$$

$$\sigma_p^2 = \frac{x_2^{\,2}-x_1^{\,2}}{(x_2-x_1)^2}(a^2+1)\sigma_{xy}^2$$

$$\sigma_b^{2^*} = \frac{2(b^{*2}+1)}{(y_2-y_1)^2}\sigma_{xy}^2$$

$$\sigma_q^{2^*} = \frac{y_2^{\,2}-y_1^{\,2}}{(y_2-y_1)^2}(q^{*2}+1)\sigma_{xy}^2 \qquad (6)$$

σ^2_{xy} is the variance of photo coordinates.

The six unknown exterior orientation parameters of a digital image are included in Equations (3 or 4). Those equations can be used to solve the unknowns. However, the equations are non-linear with respect to the parameters. Thus, linear forms are derived using the Taylor series, and an iterative approach is necessary to solve these parameters. The set of error equations provided by linearization can be written in vector form as $V = AX + L$, where V is the residual error vector, L is the vector with respect to observations, A is the design matrix with respect to parameters and X is the correction vector. In the line-based coplanarity equation a and p or b and q are observations and X_o, Y_o, Z_o, κ, φ, ω are parameters in least-squares adjustment to be determined.

2.4. Relational matching algorithm

The automatic correspondence process between the extracted straight lines in the laser intensity and in the digital frame image requires some tasks: Firstly, the extracted straight lines in the laser cloud points are projected onto the reference space (similar to the image space) using the collinearity equations (see (Mikhail et al., 2001)), IOP and the approximated EOP estimated previously. Secondly, the relational matching algorithm automatically establishes correspondences of straight lines extracted in the digital image with the projected GCL. The relational description can be established using the properties and the mutual relations between the straight lines in both spaces (image and reference space). The relational matching algorithm implemented is based on a graph (G=(N,A)), which, in its basic form, is composed of nodes and arcs, where N is the set of nodes and $A \subset N$xN is the set of arcs of G.

For each straight line in the reference space (composed by S straight lines), a search process in the image space (composed by P straight lines) is performed. The ordered sets of reference straight lines and image straight lines given by R_r and R_i, can be given by:

$$R_r = \{k_1, k_2, .., k_s\} \qquad (7)$$
$$R_i = \{e_1, e_2, .., e_P\}$$

Note that k_i denotes the i-th GCL, for $i=1,..,S$, and e_j is the j-th straight line in the image space, for $j=1,..,P$, respectively.

Now, let us define the set of binary relations between two straight lines (r) as:

$$r(k_s,k_p) = \{ r_i(k_s,k_p) |\ k_s,k_p \in R_r\},\ i=1,..,N_b$$
$$r(e_o,e_q) = \{ r_i(e_o,e_q) |\ e_o,e_q \in R_i\},\ i=1,..,N_b \qquad (8)$$

where N_b is the number of binary relations and r_i indicates the i-th binary relation. The binary relations between straight lines can be obtained by using attributes. In this work we suggest four attributes to express the binary relations between straight lines. Figure 2 shows the attributes used in this work.

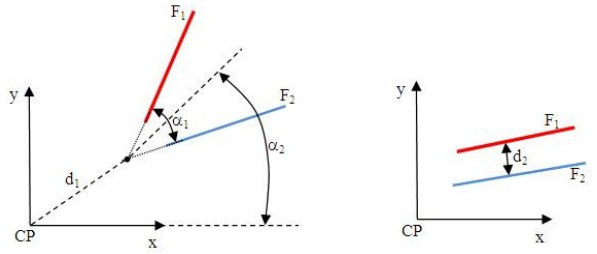

(a) (b)

Figure 2: Attributes used to express the binary relations. (a) Three attributes proposed by (Dal Poz and Tommaselli, 1996). (b) The fourth proposed attribute, used only after the fifth positive correspondence is established.

In Figure 2, x and y are the coordinates in the image space; α_1 is the angle between two straight lines F_1 and F_2, α_2 is the angle bisector, d_1 is the length from the intersection between F_1 and F_2 to the origin, d_2 is the minimum distance between two straight lines.

The attribute d_2 is applicable only after the fifth positive correspondence is established, because after that, the attributes α_1, α_2 and d_1 are not efficient as the straight lines become parallel due to the convergence in the estimated EOP with the IEKF. Considering that, a relation vector between two straight lines can be written as follows:

$$R = \{F_1, F_2, \alpha_1, \alpha_2, d_1, d_2\} \qquad (9)$$

Therefore, a relational description is a subset of binary relations with attributes given by:

$$rd_r = \{R^1_r, R^2_r, .., R^n_r\} \qquad (10)$$
$$rd_i = \{R^1_i, R^2_i, .., R^m_i\} \quad n, m=1,..,N_b$$

where rd_r and rd_i are the relational description in the reference and image space, respectively. The total relational error between the relational descriptions of straight lines in the reference and image space can be given as follows (Vosselman, 1992):

$$E(h) = \left|R_r^n \circ h - R_i^m\right| + \left|R_i^m \circ h^{-1} - R_r^n\right| + \left|R_r^{n+1} \circ h - R_i^{m+1}\right| + \left|R_i^{m+1} \circ h^{-1} - R_r^{n+1}\right| +$$
$$+ \left|R_r^n \circ h - R_i^m\right| + \left|R_i^m \circ h^{-1} - R_r^n\right| \qquad (11)$$

Note that $E(h)$ is the total error and h the mapping function between the relational descriptions. The similarity measure suggested here is an exponential function:

$$f(x) = e^{-x},\ x \geq 0 \qquad (12)$$

$x = \sum_{j=1}^{att} \left|a_i^j - a_r^j\right|$ is the similarity measure, a_i^j and a_r^j are the attributes described above; $att = \begin{cases} 3 & if \quad k \leq 5 \\ 4 & if \quad k > 5 \end{cases}$; and k is the number of positive correspondences. The relational descriptions based on straight lines are automatically constructed both in the reference and image space using a technique proposed by (Cheng and Huang, 1984). The correspondences between GCL and image straight lines are obtained by comparing the similarity measures (Equation 12).

2.5. Indirect orientation of images using GCL and iterative extended Kalman filtering (IEKF)

The Kalman filtering is a recursive solution to the discrete-data linear filtering problem, which has been used in several applications, including photogrammetric problems. In this work the indirect orientation of images is based on IEKF recursive solution presented in (Tommaselli and Tozzi, 1996). Compared to conventional least squares method, in which all observations are used simultaneously to solve a system of non-linear equations, the IEKF solution provides state updates once a new observation is available making feasible the reduction of the search space and improvement of outliers detection, reducing the probability of establishment of false correspondences.

Let $x_0 = [\kappa^0, \varphi^0, \omega^0, X_O^C, Y_O^C, Z_O^C]^T$ be the state vector with *a priori* estimate for the EOP at time t_j (see Section 2.3), ΣP_j its covariance matrix, and let lb_j^k=[*a* and *p* or *b* and *q*]^T be the observation vector for the k-th straight line extracted from image space and Σlb_j its covariance.
For each correspondence obtained between straight lines in the image space and GCLs the IEKF is applied and the data-snooping technique is used for outliers' detection (Baarda, 1968). In case no error is detected in the observations the EOP are updated, otherwise the filtered estimated are discarded. In the following iterations, the stages described above are repeated continuously until the last correspondence and the filtered state and its covariance matrix are obtained.

3. Experiments and discussions

In order to check the viability of the proposed method, some experiments with simulated and real data were performed. This section briefly summarizes the most significant results. The steps involved in the methodology were implemented in C++ using the Borland Builder 5.0 for Windows.

3.1. Data-sets used

Besides the simulated data, we used three data-sets to carry out the proposed experiments: the first one is a set of 3D coordinates of 22 ground control points (GCP) determined by means of a GPS survey; the second is one digital aerial image (with GSD around 0,4 m) acquired with a small-format digital camera Sony DSC F717, the IOP of which were previously determined with a self-calibrating bundle adjustment (BROWN, 1971); the third data-set an ALS data-set captured using an OPTECH ALTM 2050 laser scanner with an average flight height of 975 m and mean point density of 2.24 points/m^2 (~0.7 m point spacing). According to sensor and flight specifications 0.8 m horizontal and 0.25 m vertical accuracies are expected with the ALS data and an intensity image derived from ALS data-set.

The data covered part of Curitiba - more specifically the Campus of the Federal University of Paraná/Brazil.

3.2. Simulated data-set

A simulation algorithm was implemented to generate the data to perform the first experiment. Two different sets of EOP were computed using two different sets of simulated data (sets 1 and 2). The main characteristics of the numerical experiments with data-sets 1 and 2 are presented in Table 1. The simulated focal length was 10 mm and the principal point coordinates and lens distortion parameters were considered to be null.

Number of straight lines		22
standard deviation of image point coordinates x y (μm)		4.0
	Standard Deviation of object coordinates (m)	
Data-set	X Y	Z
Set 1	0.50	0.15
Set 2	0.80	0.25

Table 1: Simulated data-sets.

In Table 1 it is important to note that the main difference between these data sets are the magnitude of standard deviation introduced both in the image coordinates and object space coordinates.

For each numerical simulation nine trials were performed. Each simulation is based on normally distributed input standard deviation using the RANDG function (random errors - C++ Borland Builder 5.0). The aim of the experiments with different sets is to show the influence of image and object coordinate measurement errors in the EOP estimation. Twenty-two straight lines were simulated with different sizes and orientations and well distributed in the image. In Figure 3 the configurations of simulated straight lines are depicted.

In both data sets (1 and 2) the line parameters in the image space (*a* and *p* or *b* and *q*) were computed using the simulated image point coordinates (x y). The EOP were estimated using the line-based coplanarity model with the IEKF recursive solution. The simulated values in the set 1 represent an ideal situation, in which EOP were estimated using 3D coordinates determined by means of a GPS survey, while the set 2 represents the real situation investigated in this paper, in which the standard deviation on object coordinates corresponds to the expected ALS positional accuracy, considering the horizontal data extracted from an interpolated intensity image.

Figures 4a and 4b show the variations in the standard deviations of the estimated EOP when increasing the image and object measurement standard deviations using the values presented in Table 1 for data sets 1 and 2. The Figures 4c and 4d show the true errors computed with the simulated data.

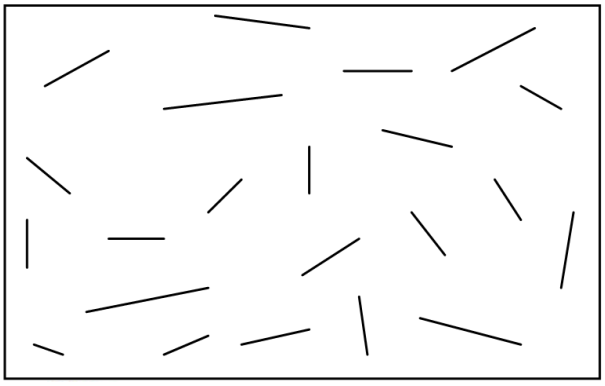

Figure 3: Configuration of simulated straight lines.

It can be noted from the analysis of Figures 4a-4d that both true errors and estimated standard deviations increase when the standard deviation is augmented, as expected. The parameter *kappa* was less affected by the standard deviation than the other angles. The computed translation errors in both experiments are similar to the accuracy in ground data used as control.
It should be noted that the image measurement accuracy (standard deviation introduced) was of 1/2 pixel (0.004 mm).

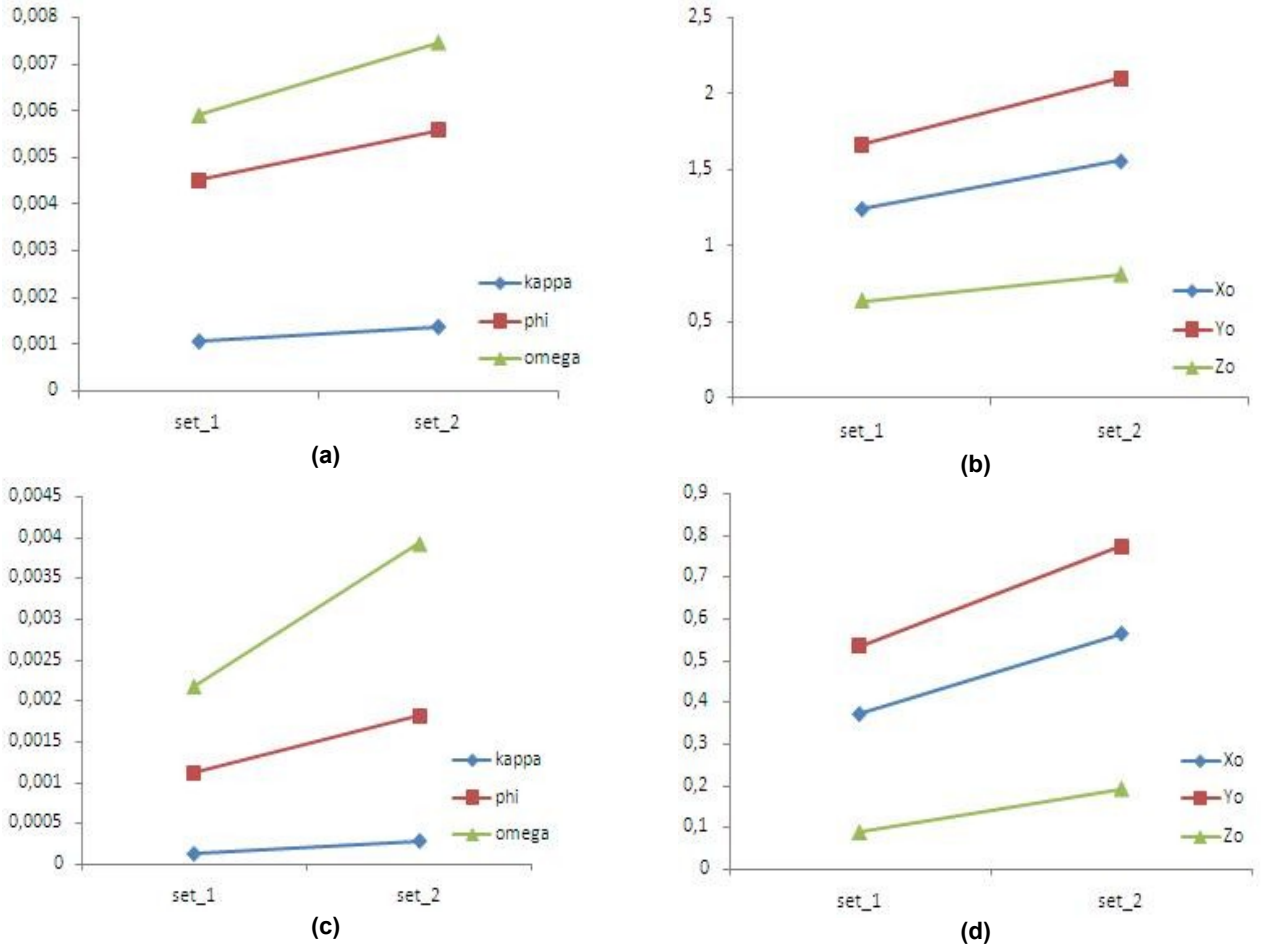

Figure 4: Results obtained from simulated data with different image and object standard deviation. **(a)** Estimated standard deviations for rotations (rad); **(b)** Estimated standard deviations for PC coordinates (m); **(c)** Computed true errors for rotations (rad); **(d)** Computed true errors for PC coordinates (m).

3.3. Verification of ALS positional accuracy

The main goal of this experiment was to assess the accuracy of ALS positional data-set (real data). We computed the discrepancies between the 3D coordinates of 22 pre-signalized points, determined by means of a GPS survey and the corresponding coordinates manually measured in the intensity image derived from ALS data-set. The Student's t-test was used to assess the accuracy of this data-set. Table 2 presents the average discrepancies, the root mean square (RMS) errors and Student's t-test (sample and calculated).
The average discrepancy and calculated Student's t-test presented in Table 2 showed that there are systematic trends for the Y components. Slightly inaccurate values of ALS bore-sight angles, as well as post-processing adjacent ALS strip adjustment, are probably the sources of this systematic error. However no final conclusions can be derived from this data and a detailed analysis of causes of this tendency is left for future work. These results demonstrated the accuracy of the ALS positional data used in the next experiment.

Number of pre-signalized GCP	22
Average discrepancy (m)	μ_X =-0.14 μ_Y=0.32 μ_Z=-0.019
Standard deviation (m)	σ_X=0.42 σ_Y=0.26 σ_Z=0.12
RMS errors (m)	RMS_X =0.45 RMS_Y=0.42 RMS_Z=0.13
Alpha	0.05
Calculated Student's t-test	t_X =-1.35 t_Y=4.98 t_Z=-0.60
Student's t-test sample	2.81

Table 2: Average, standard deviation, RMS errors and Student's t-test results.

3.4. Semi-automatic indirect orientation of an aerial image

The aim of this experiment was to compute the EOP of a digital image using the proposed method and ALS data-set. The data-set used in this experiment was composed by a single digital frame image with IOP previously determined from self-calibrating bundle adjustment and approximated EOP (calibrated focal length is 10.078 mm, average flight height ~ 730 m and pixel size 0.004 mm). The extracted straight lines in the digital and intensity images are depicted in Figure 5.

The first experiment performed was the indirect orientation using manually established correspondences between four straight lines, which were automatically extracted in the digital frame image and intensity image derived from ALS data-set. The EOPs were estimated using the line-based coplanarity model with conventional least squares adjustment.

After that first estimation step, all straight lines automatically extracted both in the image and in the object space were used for indirect orientation of the digital aerial image by using the line-based coplanarity model with the IEKF recursive solution. Table 3 shows the results obtained with the proposed method.

As expected, the estimated EOPs results achieved are affected by ALS positional data-set accuracy. The results obtained can be compared with the simulated data-set 2 (Table 1). As expected, in both cases the EOP were estimated with lower precision compared to another simulated data-set 1 with the GCPs measured directly with GPS receivers.
In this experiment, the estimated EOP were influenced by un-modelled systematic errors in the Y coordinates as well as the poor quality of X and Z coordinates both derived from ALS data-set used in this paper (~ 0.8 m and 0.25 m). The effects of the techniques to extract the GCL have to be investigated as well. Considering that the GCL have been automatically extracted in the intensity image, the Z coordinate interpolated on the raw data (derived from ALS data-set) is also affected by the horizontal uncertainty generated by the sampling in the intensity image. In this case, XYZ coordinates with larger errors than the raw data were used as endpoints of straight lines.

As described above, the results obtained in this experiment are compatible with the simulated data-set 2. Consequently, as it can be noticed in Figure 4, the proposed method has potential to achieve better results when using ALS positional data-set with better accuracy or GCL coordinates determined by means of a direct GPS survey (data-set 1 case). This can be done in a future work by using the raw data to extract the GCL, or more dense data sets.
Others topics for future work are the quality of straight lines automatically extracted in the image space and in the object space and the performance of relational matching algorithm.

It is important to emphasize that some errors in the automatic relational matching algorithm created a deficient configuration and the number of straight lines with vertical directions used in the estimation of the EOP were larger than the number of straight lines with horizontal directions. For this configuration, the Xo and *kappa* parameters achieved higher precision.

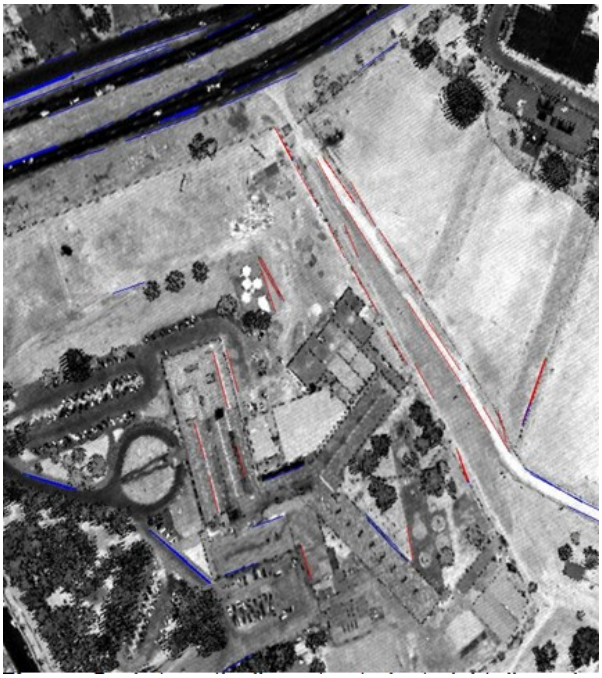

(a)

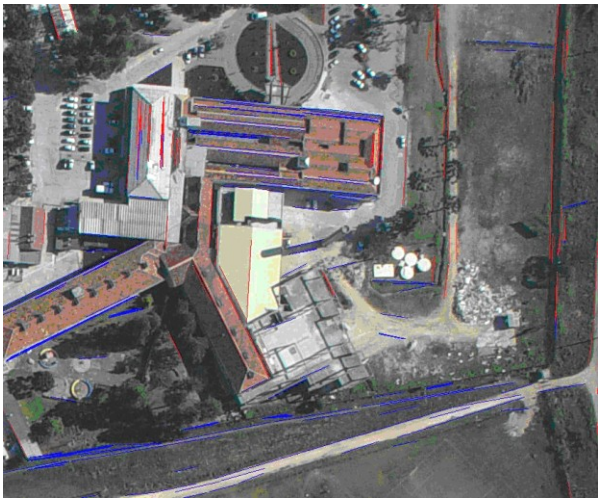

(b)

Figure 5 : Automatically extracted straight lines in a portion of the (a) digital image and (b) intensity image.

Estimated Rotations (rad)	k=1.9458 φ=-0.0024, ω=-0.017
Estimated Standard deviation of rotations (rad)	σ_k =0.00003 σ_{phy}=0.00005 σ_{omega}=0.0005
Estimated Translations (m)	Xo=7402.20 Yo=3617,22 Zo=1650.60
Estimated Standard deviation of translations (m)	σ_{Xo} =0.96 σ_{Yo}=1.52 σ_{Zo}=1.93

Table 3: Results obtained with the proposed method.

4. Conclusions

This paper experimentally assessed the potential of a semi-automatic method which uses GCL extracted from ALS data-set for indirect orientation of an aerial digital frame image. The estimation of EOP is achieved using the line-based coplanarity model with an IEKF recursive solution. Experiments with simulated and real data were conducted and the results obtained were discussed.

The assessment of the ALS positional data-set accuracy was done with a Student's t-test for the average discrepancies, showing systematic trends in the Y coordinate, which will be better investigated in a future work.

The analysis of results obtained from simulated data showed the effects of image and control standard deviation on estimated EOP values. This experiment showed that the results obtained with the proposed method, using a data-set such as simulated in the set 2, can be improved, considering data-sets with better accuracy (as the one presented in set 1).

The results obtained with real data showed that the estimation of the EOP depends on several factors, such as the performance of feature extraction and relational matching algorithms, the final configuration of the extracted GCL, the digital frame and intensity image geometric resolutions and the positional accuracy of ALS data-set. Considering the positional accuracy of the ALS data-set used, the translational parameters can be estimated with a precision around 2.0 m (for PC coordinates) and rotations typically better than 0º03'26".

An important advantage of the proposed strategy is that the restrictions on the number of GCL that can be collected no longer exist, there is no need for control points for indirect orientation of images and line-based coplanarity model does not require conjugate points and, as a result, a more robust feature matching can be used. It also offers more flexibility and greater potential for automation than point-based methods. An advantage from this paper with respect to the other researches presented is that a large number of GCL can be used, including GCL extracted from building roofs derived from ALS data-sets. This strategy improves the level of automation in the step of ground control measurement in both image and object spaces.

As disadvantages of the proposed method: the different configurations and sizes of straight lines, good initial EOP values are required when using the IEKF, robust and efficient feature extraction algorithm must be used, high geometric resolution of the intensity and digital images and scenarios with medium and highly populated urban areas must be required for good performance of the proposed approach. Also can be mentioned that the proposed method does not work in homogeneous areas, for example forests and extensive agricultural fields.

Future research will focus on the automation of the proposed method and the use of ALS positional data-set with better accuracy, basically relying on the original raw data set. Finally, it is intended to use this approach for the refinement of EOPs determined directly by GPS and INS. The use of other estimation techniques, instead of the IEKF, will be also considered in future work.

Acknowledgements

The authors would like to thank the LACTEC for providing the ALS data-set used in this paper and to the CNPq (*Conselho Nacional de Desenvolvimento Científico e Tecnológico*) for general support of this project (grant no. 570316/2008-1). Finally, we wish to thank the anonymous reviewers for their thoughtful recommendations to improve the quality of the paper.

References

Baarda, W., 1968. A Testing Procedure for Use in Geodetic Networks. New Series, vol.2, no. 5, Delft, The Nederlands.

Brown, D., 1971. Close-Range Camera Calibration. Photogrammetric Engineering and Remote Sensing 37(8), 855-866.

Cheng, L.K., Huang, T.S., 1984. Image registration by matching relational structures. Pattern Recognition 17 (1), 149-159.

Dal Poz, A. P., Tommaselli, A. M. G., 1998. Automatic absolute orientation of scanned aerial photographs. In: Anais do X SIBGRAPI, Rio de Janeiro, Brazil, pp. 1-8.

Forhuo, E., King, B., 2004. Automatica fusion of photogrammetric imagery and laser scanner point clouds. International Archives of Photogrammetry and Remote Sensing and Spatial Information Sciences XXXV (Part 3), 921-926.

Habib, A., 1999. Motion parameters estimation by tracking stationary three-dimensional straight lines in image sequences. ISPRS Journal of Photogrammetric and Remote Sensing 53 (2), 174-182.

Habib, A., Ghanma, M.S., Morgan, M.F., Mitishita, E.A., 2004. Integration of laser and photogrammetric data for calibration purposes. International Archives of Photogrammetry, Remote Sensing and Spatial Information Sciences XXXV (Part 2), 170-175.

Habib, A., Bang, K.I., Aldelgawy, M., Shin, S.W., and Kim, K.O., 2007. Integration of photogrammetric and LiDAR in a multi-primitive triangulation procedure. In: ASPRS Annual Conference, Tampa, FL, USA, pp. 7-11.

Heikkila, J., 1991. Use of linear features in digital photogrammetry. Photogrammetric Journal of Finland 12 (2), pp. 40-56.

Heuvel van den, F.A., 1997. Exterior orientation using coplanar parallel lines. In: 10th Scandinavian Conference on Image Analysis, Lappeenranta, Finland, pp. 71-78.

Kubik, K., 1988. Relative and Absolute Orientation Based on Linear Features. ISPRS Journal of Photogrammetry and Remote Sensing 46(4), 199-204.

Liu, Y., Huang, T,S., 1988. A Linear Algorithm for Motion Estimation Using Straight Line Correspondences. Computer Vision, Graphics, and Image Processing 44 (1) 35-57.

Liu, Y., Huang, T., Faugeras, O., 1990. Determination of camera locations from 2D to 3D line and point correspondences. IEEE Transactions on Pattern Analysis and Machine Intelligence 12 (1), 28-37.

Lugnani, J., 1980. Using Digital Entities as Control. PhD thesis. Department of Surveying Engineering. University of New Brunswick, Canada.

Mikhail, E., Bethel, J., McGlone, J.C., 2001. Introduction to Modern Photogrammetry. John Wiley & Sons, New York City, NY, USA, 479 p.

Mitishita, E.A., Habib, A., Centeno, J.A.S., Machado, A.M.L., 2008. Photogrammetric and LiDAR data integration using the centroid of a rectangular building roof as a control point. Photogrammetric Record 23(6), 19-35.

Mulawa, D.C., Mikhail, E.M., 1988. Photogrammetric Treatment of linear features. International Archives of Photogrammetry and Remote Sensing XXVII (Part 3), 383-394.

Park, S., Lee, K.M., Lee, S.U., 2000. A line feature matching technique based on an eigenvector approach. Computer Vision and Image Understanding 77(3), 263-283.

Ressl, C., Haring, A., Briese, C., Rottensteiner, F., 2006. A Concept for adaptive monoplotting using images and Laserscanner. International Archives for Photogrammetry, Remote Sensing and Spatial Information Sciences XXXVI(Part 3), 98-104.

Roberts, K.A., 1988. New Representation for a Line. In: Proceedings of IEEE International Conference on Computer Vision and Pattern Recognition, Ann Harbor, MI, USA, pp. 635-640.

Sanfeliu, A., Fu, K.S., 1983. A distance measure between attributed relational graphs for pattern recognition. IEEE Transactions on System, Man and Cybernetics 13 (3), 353-362.

Sahoo, P.K., Soltani, S., Wong, A.K.C., 1993. A Survey of Thresholding Techniques. Computer Vision, Graphics and Image Processing 41(2), 233-260.

Santos, D.R., Dal Poz, A.P., Dalmolin, Q., 2010. Indirect orientation of images using control points extracted by the means of monoplotting model. The Photogrammetric Journal of Finland 22(1), 25-43.

Schenk, T., 2004. From point-based to feature-based aerial triangulation. Photogrammetric Engineering & Remote Sensing 58(5-6),315-329.

Sonka, M., Hlavac, V., Boyle, R., 1998. Image Processing, Analysis and Machine Vision. Chapman & Hall, pp. 555, London, UK.

Tommaselli, A.M.G., Lugnani, J. B., 1988. An alternative mathematical model to the collinearity equation using straight features. International Archives of Photogrammetry and Remote Sensing XXVII (Part 3), 765-774.

Tommaselli, A.M.G., Tozzi, C. A., 1996. Recursive approach to space resection using straight lines. Photogammetric Engineering & Remote Sensing 62(1), 55-66.

Venkateswar, V., Chellapa, R., 1992. Extraction of Straight Lines in Aerial Images. IEEE Transactions on Pattern Analysis and Machine Intelligence 11(14), 14-25.

Vosselman, G., 1992. Relational matching. Lectures Notes in Computer Vision, Springer-Verlag, Berlin Heidelberg, pp.190.

Wehr, A., Lohr, U., 1999. Airborne laser scanning-an introduction and overview. ISPRS Journal of Photogrammetry and Remote Sensing 54(2/3), 68-82.

Zalmason, G., 2000. Hierarchical recovery of exterior orientation from parametric and natural 3-D curves. International Archives of Photogrammetry and Remote Sensing XXXIII (Part B2), 610-617.

Zhang, C., 2004. Towards and operation system for automated updating for road database by integration of imagery and geodata. ISPRS Journal of Photogrammetry and Remote Sensing 58(3-4), 166-186.